Exit wave reconstruction of radiation-sensitive materials from low-dose data

C. Huang, K. B. Borisenko and A. I. Kirkland

Department of Materials, University of Oxford, Parks Road, Oxford, OX1 3PH, UK.

Email: chen.huang@materials.ox.ac.uk

Abstract. We report exit wave reconstruction using a focal series of low-dose images for ZSM-5, a zeolite which has a wide range of industrial applications. The exit wave phase was successfully reconstructed showing the structure of ZSM-5 at a near-atomic resolution even though the dose in the individual images in the focal series was as low as 26 electrons/Å^2. This implementation shows the method's potential for application to other radiation-sensitive materials.

1. Introduction

With recent developments in both the instrumentation and the off-line data processing techniques it is possible to obtain structural and chemical information about materials at ever increasing level of detail. Spherical aberration, one of the main factors that limited the resolution of electron microscopes in the past, has now been used to improve the imaging contrast [1,2]. In addition, exit wave restoration has evolved into a standard *a posteriori* method that can be conveniently carried out and provide information on the complex electron wave at the exit plane of the specimen [3], thanks to the automatic data acquisition and the increasing availability of reconstruction software packages [4,5]. The retrieved exit wave should in theory contain no artifacts caused by various kinds of aberrations. Even in the era of aberration corrected TEM, exit wave reconstruction still has the potential of revealing the information that is lost with the phase during the image formation.

Radiation damage is known to be largely responsible for the limited resolution achieved in materials that are radiation sensitive. Attempts of minimising the influence of radiation damage can be roughly divided into two categories.

The first approach is to increase the resistivity of the samples against radiation damage through special sample preparation techniques. For example, in cryo-electron microscopy (cryo-EM) the damage rate of the sample is reduced by keeping the specimen at the liquid nitrogen temperature. This allows a higher total imaging dose to be used.

The second approach is associated with the properties of the illuminating electron beam, namely accelerating voltage and electron dose. There are two main mechanisms of the radiation damage, knock-on damage and radiolysis, both of which are dependent on the accelerating voltage, however, in the opposite ways. Using lower accelerating voltage generally decreases the knock-on damage, but increases the radiolysis, and vice versa. Therefore, these two kinds of damage cannot be completely eliminated solely by adjusting the accelerating voltage. Instead, optimal beam conditions need to be chosen according to the chemical bonding type in the studied materials to minimise radiation damage [6].

Regardless of what voltage the microscope is operated at, for light-element inorganic and organic materials, low-dose image acquisition is nearly a prerequisite for any high resolution images to be taken [7]. The inherent problem of low-dose imaging is that it substantially reduces the signal-to-noise ratio (SNR) as the electron dose decreases, resulting in blurred images, loss of the detailed structural information, and restricted interpretation of the experimental data. Although exit wave restoration from a focal/tilt series of images is an established off-line method for improving resolution and data interpretation for high-dose images, there are very few examples of exit wave reconstruction from low-dose images and the tested materials are not particularly easily damaged by electron beam [8]. In the present work we test the low-dose exit wave restoration on the radiation sensitive ZSM-5 aluminosilicate zeolite.

2. Experimental

2.1. Sample preparation

ZSM-5 is an MFI-type zeolite, belonging to the space group Pnma, with the cell parameters of a = 20.090 Å, b = 19.738 Å, c = 13.142 Å. The sample of ZSM-5, with a Si/Al ratio of 70 was first crushed into very fine powder in liquid nitrogen to make the particles more brittle and easier to generate sharp edges with thin areas. The powder was then dispersed in ethanol and deposited onto the TEM sample grid.

Prior to the actual TEM imaging, the specimen was left in the high vacuum column of the microscope for about 50 hours. It is believed that the residual ethanol and any adsorbed water had been eliminated from the material by the time of the TEM imaging.

2.2. Dose calibration

The imaging was carried out at 200 kV in the aberration-corrected JEOL 2200MCO TEM, equipped with a Faraday cage for the measurement of electron beam current, i. The gain of the CCD camera, g, can be calculated by the following equation,

$$g = it/ce \tag{1}$$

where t is the exposure time, c is the total counts in an image that contains the whole beam illumination, and e is the elementary charge. The calibration shows that every primary electron would generate 16.7 counts on average when the microscope is operated at 200 kV. Knowing the pixel area on the detector, a^2, the dose, D, for each image is calculated as:

$$D = gc/a^2 \tag{2}$$

2.3. Low-dose focal series image acquisition

The low-dose focal series of 21 images used in this paper was taken with the defocus ranging from -8 nm to 32 nm, with a 2 nm focal step between the adjacent images. The dose for a single image was controlled at 26 electrons/Å^2 over an exposure time of 3 s. There was a 1 s delay between each two images when the sample was still exposed to radiation. The total dose in this particular focal series was therefore approximately 720 electrons/Å^2.

The radiation damage was evident after recording several more focal series in the same area with the total dose of ~7000 elections/Å. In the FFT of the very first image the (14 0 0) spot is visible, corresponding to a distinguishable lattice spacing of 1.44 Å. In the last image of the final series, the visible spot with the highest spatial frequency was the (6 0 0) spot, corresponding to a lattice spacing of 3.35 Å.

3. Results and discussion

3.1. Exit wave reconstruction from the low-dose focal series

The low-dose high resolution image and the atomic model of ZSM-5 along with two exit wave phases reconstructed by FTSR and the real-space optimisation codes are shown in Figure 1. The multi-ring structure of ZSM-5 can be discerned in exit waves obtained by both methods.

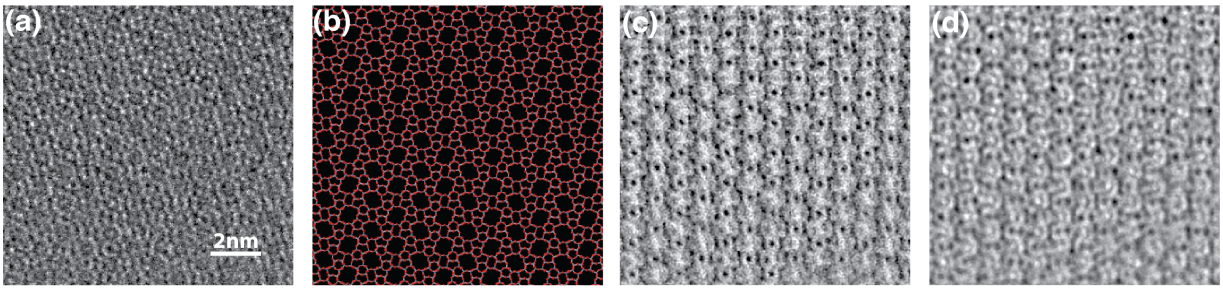

Figure 1. (a) An HRTEM image from the low-dose focal series with -2 nm defocus; (b) atomic model of ZSM-5 zeolite; (c) exit wave phases reconstructed by the FTSR plugin and (d) by the MATLAB least-squares optimisation code. The phase range is between 0 (black) ~ 0.88π (white).

3.1.1. FTSR. FTSR [4] is a commercially available DM plugin for exit wave reconstruction. It employs a phase correlation function/phase contrast index function (PCF/PCI) method for the image registration and focus determination. The registered images can then be used to restore the exit wave through a linear Wiener filter. The expected structure of ZSM-5 has larger ten-membered rings of about 9 Å in diameter, each surrounded by ten smaller rings of about 4-5 Å in diameter. The retrieved exit wave phase (Figure 1c) clearly resolved this multi-ring structure in the zeolite sample with a much lower noise level, as compared to the original image (Figure 1a).

3.1.2. MATLAB code. The real-space least-squares optimisation MATLAB code [9] uses non-linear iterative reconstruction method which integrates GPU computing to improve the performance. In the refinement process it minimises the sum of squared differences between the observed images and the images computed from the restored exit wave. The restored wave phase (Figure 1d), after filtering out the high frequency noise with a band-pass filter, gives a promising estimation of the sample structure. This method is intended for quantitative comparison with simulations. It is constrained by the quality of the initial guess from where the refinement starts and the usually finite computing power.

3.2. Image registration

A successful restoration of the exit wave needs the images in the focal series to be precisely aligned. Most of the alignment tools of EM images are based on the cross-correlation function (CCF). The FTSR software uses an enhanced phase correlation function (PCF) which includes the modulus normalisation and phase compensation for image registration. In practice, the registration result changes considerably when choosing different image slices of the series as the reference. The high noise level in the low-dose TEM images can greatly compromise the effectiveness of the image registration and is regarded as the main restriction to the quality of the exit wave restoration.

The real-space code employed a least-squares optimisation approach to the registration of images in the focal series. In addition, the corrections to the initial registration were performed after each optimisation cycle of the exit wave during the restoration.

3.3. Total dose in focal series acquisition

It must be noted that the total dose on the sample is more than just the number of images times the dose rate multiplied by the acquisition time. A considerable dose of electron irradiation the sample has been exposed to during searching and focusing processes needs to be taken into account. Although looking for a suitable area can be done at a lower magnification and the initial adjustment of focus and aberrations can be completed in adjacent areas, even then an experienced and skillful microscope operator needs time for tilting the sample to the right orientation and moving the region of interest to the optimal defocus. In reality, these two steps are not entirely independent from each other and have to be done right at the area of interest. Considering the focal series imaging, which typically takes about 1 min to collect at a constant dose, the whole preparation process before the image recording may well exceed the series imaging process in time and may be comparable in dose. Measuring this additional dose accurately will require knowledge of different fixed dose rates for searching, adjusting, and imaging, with each step precisely timed. This will be included in the future experimental design.

3.4. Defocus in the low-dose focal series

It is very challenging to identify the optimum defocus at very low doses. Therefore, even only for the purpose of getting the best contrast out of single TEM images, it is a better strategy to simply take a focal series after the coarse adjustment to the zero focus. As far as an image series for exit wave restoration is concerned, it is not a problem to have the images not equally distributed on both sides of the zero focus. The exit wave restoration software needs to be able to determine the defocus value automatically and also refine the defocus value and the focal step for more accurate restoration. These steps were implemented in the MATLAB least-squares optimisation code.

4. Conclusions

We have shown that exit wave reconstruction using low-dose focal series images is possible on an example of a radiation-sensitive ZSM-5 zeolite even when the imaging dose is as low as only 26 electrons/Å^2 per image.

Further improvement in image registration of the low-dose focal series and restoration algorithms are in progress to increase the accuracy of restoration to a level suitable for more detailed and direct comparison with the simulations.

References

[1] Haider M, Uhlemann S, Schwan E, Rose H, Kabius B and Urban K 1998 *Nature* **392** 768–9
[2] Chang L-Y, Chen F-R, Kirkland A I and Kai J-J 2003 *J. Electron Microscopy* **52** 359–64
[3] Kirkland A I and Meyer R R 2004 *Microsc Microanal* **10** 401–13
[4] Meyer R, Kirkland A I and Saxton W 2002 *Ultramicroscopy* **92** 89–109
[5] Ishizuka K 2006 *Microsc Microanal* **12** 1460
[6] Yoshida K and Sasaki Y 2013 *Microscopy* **62** 369–75
[7] Carlson D B and Evans J E 2012 Low-Dose Imaging Techniques for Transmission Electron Microscopy ed K Maaz (InTech) p 392
[8] Barton B, Jiang B, Song C, Specht P, Calderon H and Kisielowski C 2012 *Microsc Microanal* **18** 982–94
[9] Borisenko K B, Moldovan G, Kirkland A I, Wang A, Van Dyck D and Chen F-R 2012 *Journal of Physics: Conference Series* **371** 012057